GEOPHYSICAL RESEARCH LETTERS, VOL. 10, NO. 7, PAGES 501-504, JULY 1983

DYNAMIC COMPRESSION OF DIOPSIDE AND SALITE TO 200 GPa

Bob Svendsen and Thomas J. Ahrens

Seismological Laboratory, California Institute of Technology, Pasadena, CA 91125

Abstract. New Hugoniot data on single crystal diopside, $CaMgSi_2O_6$ (Di), suggest that transformation to a high-pressure thermomechanical state begins at ~50 GPa and is complete above 100 GPa, in agreement with other pyroxenes and silicates of geophysical interest. Comparison of the new high pressure phase (HPP) data for Di and salite, $CaMg_{0.82}Fe_{0.18}Si_2O_6$ (Sa) with appropriate mixed oxide and perovskite models implies compatibility between either model and the data. Conversely, least-squares fits to the HPP Di data favor lower (3.6 – 3.9 Mg/m^3) values of zero-pressure, room-temperature density than the models (4.0 – 4.1 Mg/m^3). Similar comments apply to porosity-corrected HPP hedenbergite (Hd) data. The HPP Di, Sa, and Hd data also imply much larger density differences between these compositions in the HPP regime (e.g., ≈0.8 Mg/m^3 between Di and Hd) than at STP (0.38 Mg/m^3). This may represent the influence of multiple transition processes (e.g., polymorphism and Fe^{2+} high-low spin) as a function of Fe content across the Di-Hd series. The new HPP Sa data closely parallel (≈0.1 Mg/m^3 less dense) the lower mantle density profile from ~90 GPa to 136 GPa. Our results are consistent with the speculations of Jeanloz and Ahrens on the possibility of significant Ca in the lower mantle.

Introduction

From the cosmochemical and geochemical perspective, uncertainty in the timing and timescale of the earth's accretion versus the final condensation of the solar nebula (e.g., Grossman and Larimer, 1974) admit the possibility that the earth's lower mantle (LM) may contain significantly more refractory material (e.g., Ca, Al phases) than implied by a chondrite model (e.g., Anderson, 1983). We have conducted high pressure shock-wave experiments on diopside, $CaMgSi_2O_6$ (Di), a refractory phase in the condensation sequence, and salite, $CaMg_{0.82}Fe_{0.18}Si_2O_6$ (Sa), to determine the physical properties of their HPP's at zero-pressure (P), room-temperature (T) and LM P, T, thereby constraining potential structure(s) and phase assemblages for these compositions. In light of the HPP hedenbergite, $CaFeSi_2O_6$ (Hd), data of Simakov et al. (1974) (corrected for porosity), the zero-P, room-T and in-situ density and elastic properties of the HPP Di-Hd system bound the corresponding LM properties. This is consistent with the speculation of Jeanloz and Ahrens (1980a) that the LM may contain large amounts of Ca. The geochemical consequences of significant refractory material in the LM (e.g., accomodation of more U and other incompatible elements into the chemical and thermal history of the earth) require attention, but will not be considered here.

Experimental

Large (average dimension 1.8x1.8x0.8 cm), euhedral crystals of essentially pure diopside (except for LGG117 & LGG130) were used in this study. Guided by the geometry of the crystals, ≈3 mm thick samples (1x1 cm) were sectioned perpendicular to [100] (a^*) for all experiments. Salite (Sa) was used in two experiments (LGG117, LGG130) to explore the possible compositional influence on shock deformation. Each experiment was performed on either a two stage, light gas gun (LGG), or a 40 mm bore, solid propellant gun (e.g., Jeanloz and Ahrens, 1977, 1980a). Tungsten (40 mm experiments) or tantalum (LGG experiments) flyer plates impacted samples at velocities (Table 1) between 1.7 and 6.6 km/sec. Impact velocities were measured directly during the 40 mm experiments and calculated from experimental dimensions and time measurements for the LGG experiments. Shock-wave transit times were determined by analysis of image-converter streak (LGG) or rotating mirror (40 mm) camera photographs, which recorded changes in the reflectivity of sample and buffer mirrors as the shock-wave passed through them. When arrival surface clarity was a problem (at least partly due to image-converter cross talk in the LGG experiments: Vassiliou and Ahrens, 1981), these records were digitized and resulting measurements fit by least-squares (LSQ) regression. Crosstalk and projectile bowing were the most significant experimental errors (≈2%) inherent in the calculated shock wave velocities, causing fuzziness or curvature, respectively, in the arrivals.

Assuming uniaxial strain, the mechanical state behind the shock front (internal energy, stress, particle velocity and density) was calculated from the measured initial density, impact velocity, and shock-wave transit time, plus the equation of state (EOS) of the flyer and driver materials, using the impedance-match technique (McQueen et al.,1970). Release states were calculated by a similar analysis for the buffer material (Lexan, ≈1.7 mm thick, and fused quartz ≈1.9 mm thick, for the 40 mm and LGG experiments, respectively). Isentropic release (Jeanloz, 1979) and the consequent Riemann integral formalism (e.g., Rice et al., 1958; Lyzenga and Ahrens, 1978) were assumed. The error analysis followed that of Jackson and Ahrens (1979).

Results

Collectively, our data and the polycrystalline data of Ahrens et al. (1966) comprise three relatively distinct groups (see Figure 1): (1) the low-P phase (LPP, 8 data) from the Hugoniot elastic limit at about 10 GPa (Ahrens et al., 1966) up to about 50 GPa, (2) a mixed phase region (MPR, 1 datum) from ~50 GPa to 100 GPa, and (3) a HPP regime ≥100 GPa. The LPP Di data (Table 1) are generally consistent with static compression results (Levien et al., 1979). The extent of LPP Di is well defined; the onset of the MPR is clearly implied by (1) shock velocity (U_s) - particle velocity (u_p) relations (Table 1), and (2) the offset of the 66 GPa datum from the metastable extrapolation of the LPP Hugoniot (Figure 1). The 3 LPP Di data from this study also have release paths subparallel to the LPP Hugoniot (Figure 1), suggesting that they are not transforming. That the transformation is occurring near 50 GPa is consistent with other pyroxenes and silicates (e.g., bronzite: Jeanloz and Ahrens, 1977; forsterite: Syono et al., 1981).

The HPP regime is represented by 3 Di data, 2 Sa data, and the 3 Hd data of Simakov et al. (1974) shown in Figure 1. One prominent feature of the HPP data is the distinct Hugoniot behavior of Di, Sa, and Hd, due in part to their different initial densities (3.28, 3.35, and 3.42 Mg/m^3, respectively). Apparently, the HPP Hd data are porous (≈6.6%) and/or contain significant Mg, since the STP "crystal" density quoted by Simakov et al. (1974) is 3.42 Mg/m^3, much less than the crystal density of Hd_{100} (3.66 Mg/m^3, calculated from the lattice parameters of Rustein and Yund, 1969). We suspect that the Hd data are porous because the transition to HPP Hd begins at ~40 GPa (and 4.5 Mg/m^3), and is complete by ~60 GPa (and 5.2 Mg/m^3), a pressure much lower than generally observed for crystalline silicates (≥100 GPa), even those

Paper number 3L0461.
0094-8276/83/003L-0461$3.00

Table 1. Experimental Conditions and Results

Shot #	Initial Density (Mg/m^3)	Impact Velocity (km/sec)	Hugoniot State: Shock Velocity (km/sec)	Hugoniot State: Particle Velocity (km/sec)	Hugoniot State: Pressure (GPa)	Hugoniot State: Density (Mg/m^3)	Release State: Shock Velocity (km./sec.)	Release State: Particle Velocity (km./sec.)	Release State: Pressure (GPa)	Release State: Density (gm./cc.)
40MM513	3.276	1.737	8.00	1.34	35.0	3.93	5.27	1.88	11.8	3.75
	(0.002)	(0.009)	(0.07)	(0.01)	(0.3)	(0.01)	(0.07)	(0.05)	(0.5)	(0.04)
40MM520	3.276	2.156	8.16	1.66	44.4	4.11	6.05	2.37	17.1	3.82
	(0.004)	(0.110)	(0.15)	(0.09)	(2.4)	(0.06)	(0.10)	(0.06)	(0.7)	(0.15)
40MM510	3.279	2.406	8.29	1.85	50.3	4.22	6.56	2.69	21.1	3.76
	(0.002)	(0.028)	(0.07)	(0.02)	(0.7)	(0.02)	(0.08)	(0.05)	(0.7)	(0.07)
LGG117	3.342	4.203	8.96	3.06	91.5	5.07	7.30	3.90	62.8	4.50
	(0.006)	(0.010)	(0.22)	(0.02)	(1.7)	(0.08)	(0.19)	(0.12)	(3.7)	(0.22)
LGG125	3.273	4.310	9.60	3.11	97.5	4.84	7.35	3.93	63.7	4.40
	(0.004)	(0.008)	(0.24)	(0.02)	(1.9)	(0.07)	(0.18)	(0.12)	(3.5)	(0.16)
LGG130	3.348	5.291	9.94	3.82	127.1	5.44	8.93	4.93	97.1	4.44
	(0.002)	(0.050)	(0.21)	(0.04)	(2.4)	(0.09)	(0.22)	(0.14)	(5.1)	(0.36)
LGG103	3.261	5.358	10.44	3.85	131.1	5.17	8.78	4.84	93.6	4.56
	(0.004)	(0.077)	(0.29)	(0.07)	(3.5)	(0.11)	(0.34)	(0.21)	(7.7)	(0.37)
LGG112	3.275	6.592	11.62	4.70	179.0	5.50	10.25	5.76	130.1	4.88
	(0.004)	(0.077)	(0.33)	(0.07)	(4.6)	(0.14)	(0.34)	(0.22)	(9.4)	(0.36)

Standard error in parentheses.
All samples are oriented perpendicular to [100].

containing mostly Fe (e.g., fayalite: Vassiliou and Ahrens, unpublished data). The much higher degree of irreversible heating produced in shock-compressed porous versus nonporous materials reduces the kinetic resistance of the lattice to completion of the transition, resulting in a less extensive MPR. Note that the MPR of (nonporous) Di (Figure 1) extends from ~50 to 100 GPa (and ~4.3 to 5.3 Mg/m^3). Porosity corrections (e.g., Al'tshuler et al., 1965) applied to these Hd data yield curve 5 in Figure 1.

In order to compare the HPP Di, Sa, and Hd data to potential LM mixed oxide (MO) or PV assemblages, models were constructed from appropriate end-member EOS parameters (Table 2) by volume (density and MO γ_o) and VRH (K_{os}, K'_{os}) averaging. The parameters for $FeSiO_3$(pv) are hypothetical in the sense that $FeSiO_3$(pyx) apparently transforms into a MO assemblage of FeO(?) + SiO_2(st) under LM conditions (Liu, 1976).

The bounds of the models (e.g., HPP Di, Figure 2) imply that HPP Di, Sa, and Hd are consistent with either MO or PV phase assemblages. Work by Mao et al. (1977) and Liu (1979) implies that Di transforms at ~20 and 800°K to a $MgSiO_3$ perovskite phase and a nonquenchable phase thought to be $CaSiO_3$ cubic perovskite. Assuming the Di datum near 95 GPa is completely transformed, a LSQ best fit to the HPP Di data implies a significant discrepancy between the zero-P densities of the best fit and the models. Similar comments apply to the HPP Sa data and corrected HPP Hd data of Simakov et al. (1974).

Discussion

Most work concerning the composition of the LM (e.g., Watt and O'Connell, 1979; Watt and Ahrens, 1982a) has focused almost exclusively on various Mg, Fe oxide and/or silicate assemblages. This attention has been motivated primarily by the strong appeal of (1) the consistency of solar and C1 carbonaceous chondrite bulk compositions, coupled with a dominantly homogeneous accretion history for the earth, and (2) the apparent consistency of purely Mg, Fe silicate models and seismic ρ, K profiles of the LM. Gaffney and Anderson (1973) objected to Ca being a significant component of the LM because of the low zero-P density (3.97 Mg/m^3) they calculated for the most likely phase, $CaSiO_3$(pv). This objection was removed by the work of Liu and Ringwood (1975), which implied a zero-P density for $CaSiO_3$(pv) of 4.17 ± 0.6 Mg/m^3 (Table 2). Jackson and Ahrens (1979) considered a pyrolite model for D" (at 120 GPa, based on shock-wave data) containing ≈6.4 wght.% $CaSiO_3$ and concluded that it was marginally compatible with the range of possible densities for D" at that pressure constrained by seismic models. Ruff and Anderson (1980) constructed pyrolite (≈3.8 wght.% CaO) and "refractory" (≈33 wght.% CaO and 21 wght.% Si depletion) models for D" from shock-wave data and concluded that a refractory D" would be ~0.1 Mg/m^3 denser than a pyrolite D" at 120 GPa (although they overlap within stated uncertainties). Ruff and Anderson (1980) also estimated the seismic parameter $\Phi = V_\phi^2$ of $CaSiO_3$(pv) to be 52 km^2/sec^2, consistent with the parameters listed in Table 2 for this material. This estimate implies that V_ϕ of D" would be significantly lower than "normal mantle" (Ruff and

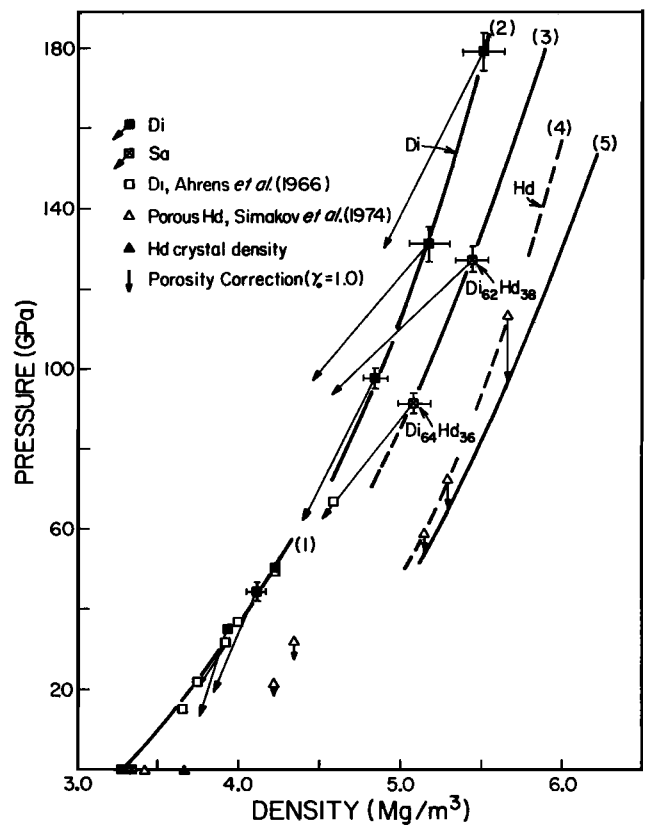

Fig. 1. Pressure - density relations for LPP $CaMgSi_2O_6$ (Di, curve 1), HPP Di (curve 2), $CaMg_{0.82}Fe_{0.18}Si_2O_6$ (Sa, curve 3) and $CaFeSi_2O_6$ (Hd, curve 4; porosity correction, curve 5). Curve 1 is an unconstrained LSQ best fit to the LPP Di data. Curves 2-5 were constructed using the shockwave EOS to interpolate between respective data points shown.

Table 2. End Member Equation of State Parameters and MO and PV Models for Di and Hd compositions

End members	ρ_o (gm./cc.)	K_o (GPa)	K_o	γ_o
CaO(B2)[1]	3.76	115.0	4.9	1.8
	(0.05)a	(8.0)	(0.2)	(0.2)
FeO(?)[1]	6.05	195.0	3.4	1.8
	(0.15)	(10.0)	(0.5)	(0.2)
MgO(B1)[2]	3.583	163.0	4.2	1.5
	(0.02)	(1.0)	(0.2)	(0.5)
SiO_2(st)[3]	4.29	316.0	4.0	1.5
		(4.0)	(1.0)	(0.5)
$CaSiO_3$(pv)[4]	4.13	220.0	4.0	1.2 b
		(20.0)	(1.0)	(0.5) b
$FeSiO_3$(pv)[5]	5.23	250.0	4.0	1.2
		(20.0)	(1.0)	(0.5)
$MgSiO_3$(pv)[6]	4.10	260.0	4.0	1.2
		(20.0)	(1.0)	(0.5)
Models				
$CaMgSi_2O_6$(mo)	4.00	207.5	4.2	1.6
		(26.2) c	(0.7)	(0.2)
$CaMgSi_2O_6$(pv)	4.12	237.7	4.0	1.2
		(20.0)	(1.0)	(0.5)
$CaFeSi_2O_6$(mo)	4 53	214.2	4.0	1.6
		(27.5)	(0.8)	(0.3)
$CaFeSi_2O_6$(pv)	4.65	233.6	4.0	1.2
		(19.3)	(1.0)	(0.5)

[a] standard error of experiment.
[b] assumed for all pv γ_o.
[c] standard deviation of mean and error of experiment.
[1] Jeanloz and Ahrens (1980a).
[2] Vassiliou and Ahrens (1981).
[3] Weidner et al. (1982).
[4] ρ_o from Liu and Ringwood (1976); K_{os} estimated from methods of Liebermann et al. (1977).
[5] ρ_o estimated from extrapolated lattice parameters of hypothetical pv phase: Yagi et al. (1979a); K_{os} estimated as in [4].
[6] Yagi et al. (1979a, 1979b).

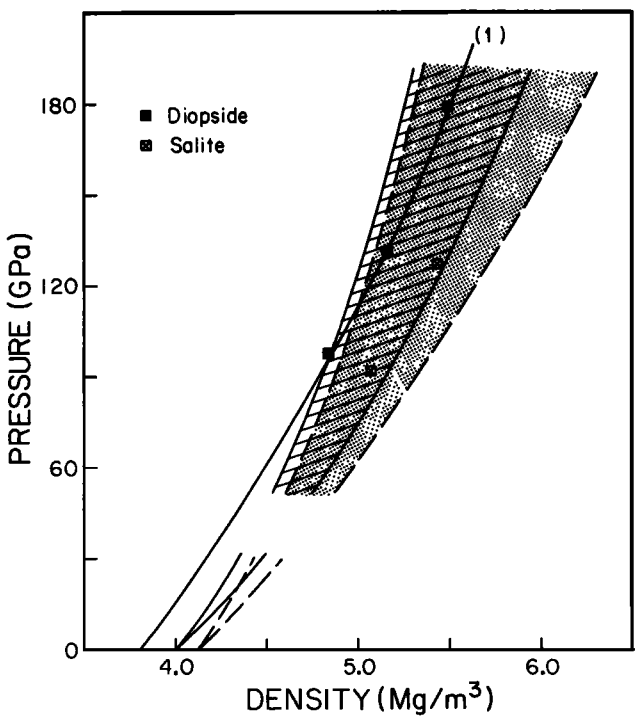

Fig. 2. Comparison of the HPP Di data with a range of theoretical hugoniots constructed from MO (unbroken curve) and PV (dashed curve) models (Table 3) for this composition. Each field represents the experimental plus standard uncertainty in model EOS parameters. For comparison, note curve 1, an example of a LSQ best fit (centered at e_{tr} of 1.0 MJ/kg) to the HPP Di data.

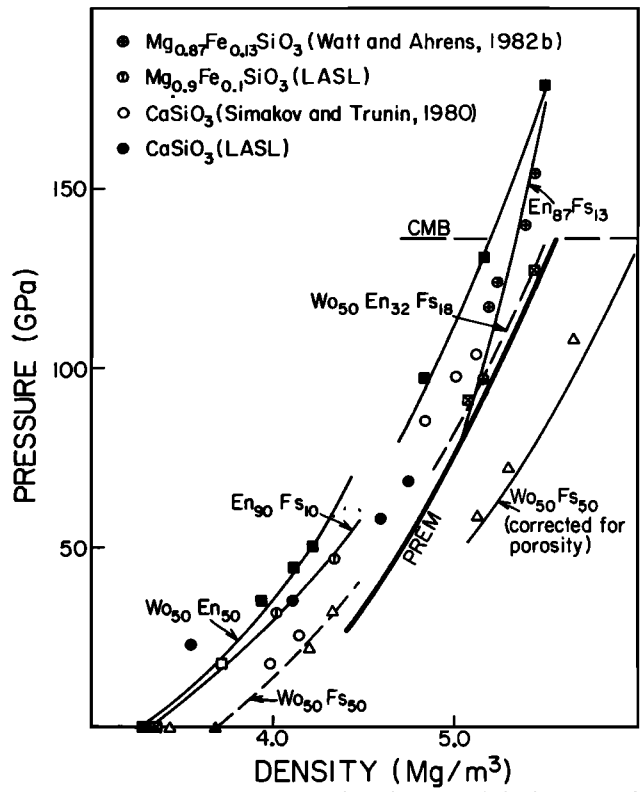

Fig. 3. Pyroxene end-member Hugoniot relations and the lower mantle pressure-density profile of PREM. Hugoniot relations for the solid-solution series $CaMgSi_2O_6$ - $CaFeSi_2O_6$ parallel the seismic density profile throughout the lower mantle, while those of En_{87} (Watt and Ahrens, 1982c) are much steeper. Also note that HPP Sa ($Wo_{50}En_{32}Fs_{18}$) closely follows the seismic density profile throughout the lower mantle.

Anderson, 1980, estimate ~8% less for their refractory model) if it contain large amounts of $CaSiO_3$(pv). At this point, the behavior of V_ϕ in D" is unclear; in light of the work of Ruff and Helmberger (1980) and Lay and Helmberger (1982), it may decrease through D".

Ideal mixing of zero-P, room-T densities and bulk moduli for HPP Di (3.6-3.9 Mg/m^3 and 200-300 GPa, respectively, LSQ fits) and HPP Hd (4.3-4.6 Mg/m^3 and 190-280 GPa, respectively, LSQ fits to corrected data) constrained to satisfy the corresponding LM properties (4.19 Mg/m^3 and 236 GPa, respectively: Stacey et al., 1981) imply x_{Hd} ~0.4–0.6 (mass fraction). If the MO or PV models are representative of HPP Di and Hd, then MO x_{Hd} ~0.41 and PV x_{Hd} ~0.14. A number of studies (e.g., Watt and Ahrens, 1982a; Anderson, 1983) favor a pyroxene stoichiometry for the LM. Our results suggest the trade-off between Ca and Fe on density and elastic properties implied by crystal systematics (Shankland and Chung, 1974), although for elastic properties, perhaps not by the data (Weidner and Vaughan, 1982).

Lastly, we consider a compendium of selected pyroxene Hugoniot relations and the LM, represented in Figure 3. Thermostatic Hugoniot temperature calculations suggest a temperature range of ~700–3000°K for Di and ~1500–5000°K for (corrected) Hd in the mantle pressure range 50 to 136 GPa. Presumably HPP Sa lies between these estimates. Given a range of LM temperature profiles, bounded above by Stacey (1977) and below by Brown and Shankland (1981), raw HPP Di and Hd data are then consistent with LM temperatures from ~90 to 136 GPa and 80 to 100 GPa, respectively. Note that the Hugoniot of Di and Hd (as well as that of Sa) apparently parallel the PREM (Dziewonski and Anderson, 1981) profile throughout the LM, while that of En_{87} (Watt and Ahrens, 1982b) is much steeper. The position of the HPP Sa data are much denser (≈20%) than

expected from ideal mixing of HPP Di and Hd. Also, note that the in-situ density range of the HPP Di-Hd system is significantly (≈40%) larger than that of the LPP. These observations, coincident with the increase of Fe^{2+} across the system, suggest that a high-low spin transition, as well as a polymorphic transition, may be involved in the transformation of members of the Di-Hd system with significant (perhaps as little as 18 mole %: Sa data) Fe^{2+}. For FeO, Jackson and Ringwood (1981) conclude that this type of transition is most likely in the 50-90 GPa range and produces a further 10-16% increase in zero-P density. Our LSQ fits to the HPP Di-Hd data imply a 10-20% difference in zero-P density across this system, as opposed to 10.4% for the LPP. Thus our data are marginally compatible with the possible further density change implied by the FeO results.

Acknowledgements. We thank E. Gelle, M. Long, W. Ginn and their assistants, whose experimental expertise make our work at the Lindhurst Lab possible. We thank M. S. Vassiliou and J. Bass for reviewing an earlier version of this manuscript and making many helpful suggestions. M. S. Vassiliou, J. Bass, M. Boslough and D. L. Anderson provided helpful discussions. We are indebted to S. Huebner (USGS, Reston, VA) for providing diopside samples. Support was provided by the National Science Foundation, grant #EAR 80-18819. Contribution #3877, Division of Geological and Planetary Sciences, California Institute of Technology.

References

Ahrens, T. J., Rosenburg, J. T., and M. H. Ruderman, Dynamic properties of rocks, *Stanford Research Institute, Final Report*, DA-45-146-XZ-277, SRI Project FGU-4816, Sept. 1966.

Al'tshuler, L. V., Trunin, R. F., and G. V. Simakov, Shock-wave compression of periclase and quartz, and the composition of the earth's lower mantle, *Izv. Acad. Sci. USSR, Phys. Sol. Earth*, 657-660, 1965.

Anderson, D. L., Chemical composition of the mantle, submitted to *Geophys Res. Lett.*, 1983.

Brown, J. M., and T. J. Shankland, Temperature profile of the lower mantle calculated from seismological data, *Geophys. J. R. astr. Soc.*, V. 66, 579-596, 1981.

Dziewonski, A. M., and D. L. Anderson, Preliminary reference Earth model, *Phys. Earth Planet Int*, V. 25, 297-356, 1981.

Gaffney, E. S., and D. L. Anderson, Effect of low-spin Fe^{2+} on the composition of the lower mantle, *J. Geophys. Res.*, V. 78, 7005-7014, 1973.

Grossman, L., and J. W. Larimer, Early chemical history of the solar system, *Rev. Geophys. Space Phys.*, V. 12, 71-101, 1974.

Jackson, I. A., and T. J. Ahrens, Shock-wave compression of single-crystal forsterite, *J. Geophys. Res.*, V. 84, 3039-3048, 1979.

Jackson, I. A., and A. E. Ringwood, High pressure polymorphism of the iron oxides, *Geophys. J. R. astr. Soc.*, V. 64, 767-783, 1981.

Jeanloz, R., Release adiabat measurements on minerals: The effect of viscosity, *J Geophys. Res.*, V. 84, 7545-7548, 1979.

Jeanloz, R., and T. J. Ahrens, Pyroxene and Olivine: Structural implications of shock-wave data for high pressure phases, in *High Pressure Research: Applications in Geophysics*, M. H. Manghnani and S. Akimoto, eds., Academic Press, New York, NY, 642 pp., 1977.

Jeanloz, R., and T. J. Ahrens, Equation of state of FeO and CaO, *Geophys J. R. astr. Soc.*, V. 62, 505-528, 1980a.

Lay, T., and D. V. Helmberger, A lower mantle S wave triplication and the shear velocity structure of D", Submitted to *Geophys. J. R. astr. Soc.*, 1982.

Levien, L., Weidner, D. J., and C. T. Prewitt, Elasticity of diopside, *Phys. Chem. Minerals*, V. 4, 105-113, 1979.

Liebermann, R. C., Jones, L. E. A., and A. E. Ringwood, Elasticity of aluminate, titanate, stannate and germanate compounds with the perovskite structure, *Phys. Earth Planet. Int.*, V. 14, 165-178, 1977.

Liu, L. G., The high pressure phases of $FeSiO_3$ with implications for Fe_2SiO_4 and FeO, *Earth Planet. Sci. Lett.*, V. 33, 101-106, 1976.

Liu, L. G., The system enstatite-wollastonite at high pressures and temperatures, with emphasis on diopside, *Phys. Earth Planet Int.*, V. 19, P15-P18, 1979.

Liu, L. G., and A. E. Ringwood, Synthesis of a perovskite-type polymorph of $CaSiO_3$, *Earth Planet. Sci. Lett.*, V. 28, 209-211, 1975.

Lyzenga, G. A., and T. J. Ahrens, The relation between shock-induced free surface velocity and post-shock density of solids, *J. Appl. Phys.*, V. 49, 201-204, 1978.

Mao, H. K., Yagi, T., and P. M. Bell, Mineralogy of the Earth's deep mantle: quenching experiments on mineral compositions at high pressures and temperatures, in *Carnegie Institute of Washington Yearbook* 77, 502-504, 1977.

Marsh, S. P., LASL shock Hugoniot data, University of California at Berkeley Press, Berkeley, CA, 1980.

McQueen, R. G., Marsh, S. P., Taylor, J. W., Fritz, J. N., and W. J. Carter, The equation of state of solids from shock-wave studies, in *High Velocity Impact Phenomena*, 294-419, R. Kinslow, ed., Academic Press, New York, NY, 1970.

Rice, M. H., McQueen, R. G., and J. M. Walsh, Compressibility of solids by strong shock waves, *Solid State Physics*, V. 6, 1-63, 1958.

Ruff, L. J., and D. L. Anderson, Core formation, evolution and convection: a geophysical model, *Phys. Earth Planet. Int.*, V. 21, 181-201, 1980.

Ruff, L. J., and D. V. Helmberger, The structure of the lowermost mantle determined by short-period P wave amplitudes, *Geophys. J. R. astr. Soc.*, V. 68, 95-119, 1981.

Rustein, M. S. and R. A. Yund, Unit cell parameters of synthetic diopside-hedenbergite solid solutions, *Am. Mineral.*, V. 54, 238-245, 1969.

Shankland, T. J., and D. H. Chung, General relationships among sound speeds, II. Theory and discussion, *Phys Earth Planet. Int.*, V. 8, 121-129, 1974.

Stacey, F. D., A thermal model for the earth, *Phys Earth Planet. Int.*, V. 15, 341-348, 1977.

Stacey, F. D., Brennan, B. J., and R. D. Irvine, Finite strain theory and comparisons with seismological data, *Geophys. Surv.*, V. 4, 189-232, 1981.

Simakov, G. V., Pavlovsky, M. N., Kalashinkov, N. G., and R. F. Trunin, Shock compressibility of twelve minerals, *Izv Earth Phys.*, V. 8, 11-17, 1974.

Simakov, G. V., and R. F. Trunin, The compression of minerals by shock waves, *Izv Earth Phys*, V. 16, 134-137, 1980.

Syono, Y., Tsuneaki, G., Sato, J., and H. Takei, Shock compression of single-crystal forsterite in the pressure range 15-93 GPa, *J. Geophys. Res.*, V. 86, 6181-6186, 1981.

Vassiliou, M. S., and T. J. Ahrens, Equation of state of periclase to 200 GPa, *Geophys. Res. Lett.*, V. 8, 729-732, 1981.

Watt, J. P., and R. J. O'Connell, Mixed-oxide and perovskite-structure model mantles from 700-1200 km, *Geophys. J. R. astr. Soc.*, V. 54, 601-630, 1979.

Watt, J. P., and T. J. Ahrens, The role of iron partitioning in mantle composition, evolution and scale of convection, *J. Geophys Res.*, V. 87, 5631-5644, 1982a.

Watt, J. P., and T. J. Ahrens, Shock-wave equation of state of enstatite (abs.), *EOS*, V. 63, 1097, 1982b.

Watt, J. P., and T. J. Ahrens, Dynamic compression of forsterite, Submitted to *J. Geophys Res.*, 1982c.

Weidner, D. J., Bass, J. D., Ringwood, A. E., and W. Sinclair, The single crystal elastic moduli of stishovite, *J. Geophys. Res.*, V. 87, 4740-4746, 1982.

Weidner, D. J., and M. T. Vaughan, Elasticity of pyroxenes: effects of composition and crystal structure, *J. Geophys Res*, V. 87, 9349-9353, 1982.

Yagi, T., Mao, H. K., and P. M. Bell, Lattice parameters and specific volume for the perovskite phase of orthopyroxene composition $(Mg,Fe)SiO_3$, in *Carnegie Institute of Washington Yearbook* 78, 612-613, 1979a.

Yagi, T., Mao, H. K., and P. M. Bell, Hydrostatic compression of $MgSiO_3$ of perovskite structure, in *Carnegie Institute of Washington Yearbook* 78, 613-614, 1979b.

(Received February 18, 1983;
accepted March 11, 1983.)